Original research article

EJO European Journal of Ophthalmology

European Journal of Ophthalmology
2020, Vol. 30(6) 1397–1402

DOI: 10.1177/1120672119873210
journals.sagepub.com/home/ejo


Ultra-wide-field imaging of choroidal melanoma before and after proton beam radiation therapy

Angeliki Psomiadi[1], Gertrud Haas[1], Michael Edlinger[2], Nikolaos E Bechrakis[3] and Georgios Blatsios[1]

Abstract

Objective: To evaluate the imaging characteristics of choroidal melanoma before and after proton beam radiotherapy via Optos® ultra-wide-field scanning laser ophthalmoscopy.

Methods: Retrospective, descriptive study of choroidal melanoma patients treated with proton beam radiotherapy. All patients underwent full clinical evaluation, including best-corrected visual acuity, ultrasound examination and ultra-wide-field scanning laser ophthalmoscopy imaging in the pseudo-colour (red and green channel) as well as autofluorescence mode. Tumours were classified and evaluated according to their location, size, presence of subretinal fluid, drusen, orange pigment and reflectance intensity in ultra-wide-field scanning laser ophthalmoscopy. Tumour sonographic (basal diameter, height) and ultra-wide-field scanning laser ophthalmoscopy imaging dimensions (maximal diameter) were documented.

Results: A total of 39 eyes (38 patients) were followed for 24 months (range 6–48 months). Mean best-corrected visual acuity dropped from 20/40 to 20/63 after proton beam radiotherapy. There was no change in the imaging tumour characteristics during follow-up. Subretinal fluid changes were better detected in the autofluorescence compared to pseudo-colour mode. Mean tumour diameter did not significantly change in the ultra-wide-field scanning laser ophthalmoscopy although it did so in the ultrasound. No patient showed local tumour recurrence.

Conclusion: The ultra-wide-field scanning laser ophthalmoscopy imaging characteristics of choroidal melanoma in the Optos® system do not significantly change after proton beam radiotherapy after a mean follow-up of 2 years.

Keywords

Choroidal melanoma, ultra-wide-field imaging

Date received: 4 March 2019; accepted: 10 August 2019

Introduction

Choroidal melanoma is the most common primary malignant intraocular tumour in the adult population.[1] Proton beam radiotherapy (PBRT) is one valuable treatment option for choroidal melanoma,[2] especially for large or posterior tumours close to the macula or the optic disc.[3] As in other radiation methods, factors that can negatively influence the visual outcome after PBRT are radiation retinopathy, maculopathy, optic neuropathy and toxic tumour syndrome.[4]

Photographic documentation and ultrasound scanning are important tools for the follow-up of intraocular neoplasms. One of the most commonly used system for ultra-wide-field scanning laser ophthalmoscopy (UWF-SLO) is the Optos® (Optos PLC, Dunfermline, Scotland). It uses two laser wavelengths: a green wavelength (532 nm), which delivers images of the retina surface and its

[1]Department of Ophthalmology, Medical University Innsbruck, Innsbruck, Austria
[2]Department of Medical Statistics, Informatics, and Health Economics, Medical University Innsbruck, Innsbruck, Austria
[3]Department of Ophthalmology, University Hospital Essen, Essen, Germany

Corresponding author:
Georgios Blatsios, Department of Ophthalmology, Medical University Innsbruck, Anichstrasse 35, 6020 Innsbruck, Austria.
Email: georgios.blatsios@gmail.com

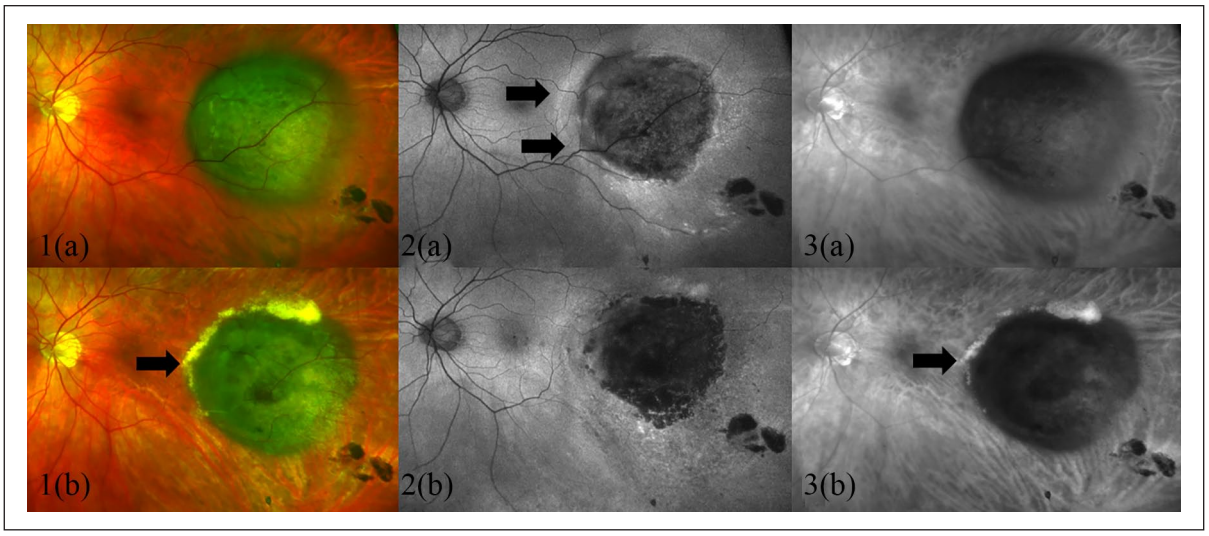

Figure 1. Images of the same patient with choroidal melanoma before (a) and after (b) proton beam radiotherapy (last follow-up 32 months). 1(a) and (b): pseudo-colour mode, pigmented tumour; the arrow indicates lipid exudation. 2(a) and (b): autofluorescence, mixed tumour; the arrows indicate the presence of subretinal fluid (confirmed by spectral-domain optical coherence tomography). 3(a) and (b): red channel, mixed tumour; the arrow indicates lipid exudation.

vasculature (green channel), and a red wavelength (633 nm), which penetrates the deeper layers of the retina and the choroid (red channel). The combination of these two wavelengths results in a pseudo-colour image. It is also capable of obtaining auto-fluorescence (AF) images using the green laser of 532 nm for excitation and a 570–780 nm emission filter, as a result it is less influenced by cataract.[5–7] A typical high-resolution scan can be obtained in a fraction of second, thus reducing motion artefacts.

Due to the design of the mirrors in the Optos, the lesion resolution in pixels depends on its anterior-posterior location.[8] Peripheral images can be magnified and the horizontal axis appears stretched compared with vertical axis.[9]

Several studies have used these Optos utilities for documenting and differentiating choroidal and retinal lesions to enhance diagnosis of choroidal tumours.[10–15] Our study, in contrast, is evaluating tumour characteristics documented on Optos® images before and their changes after PBRT.

Methods

Aim of this study was to focus on the imaging of characteristics of uveal melanomas before and after PBRT. This is crucial because clinicians are confronted with the question whether a change or no change of the imaging characteristics after PBRT suggest local tumour control or not. The study adhered to the tenets of the Declaration of Helsinki and was approved by the Ethics Committee of the Medical University Innsbruck, Austria. It is a retrospective study that included 38 patients diagnosed with choroidal melanoma and treated PBRT at the Helmholtz Centre in Berlin, Germany and at Paul Scherrer Institute in Switzerland between October 2008 and October 2016. One of our patients had bilateral choroidal melanoma; we listed the investigated characteristics from both eyes as separate. Thus a total of 39 tumours were included in our study. All patients received tantalum clip implantation surgery in our department prior to PBRT. The treatment protocol consisted of a total radiation dosage of 60 Gy delivered in four sessions of 15 Gy each over four consecutive days. Exclusion criteria for our study were: surgical resection after radiation, ciliary body melanomas and initial fundus colour imaging with camera systems other than Optos®. The fundus imaging system used was OPTOS® 200 Tx (Optos PLC, Dunfermline, Scotland). It offers images using multiple wavelengths, including options for pseudocolour, red channel, green channel, fluorescein angiography and AF with a view of the retina over 200° with a single capture. Each channel was viewed separately and analysed with the Optomap Vantage V2 Software with ProView™ option, which minimises distortion and magnification irregularities.[16]

The following data were evaluated (pre-treatment and at the last follow-up visit): Snellen visual acuity (hand perception was noted as 20/2000), tumour location as well as post PBRT retinopathy (telangiectasias, microaneurysms, neovascularisation, vitreous haemorrhage, hard exudates, cotton wool spots, retinal edema) (Figure 1); maculopathy (macular edema); optic neuropathy (pale optic disc, disc edema along with haemorrhage and microangiopathy); and toxic tumour syndrome (all of the above plus exudative retinal detachment and/or rubeosis iridis and neovascular glaucoma).[4]

A number of parameters on the Optos images were documented (Table 1). Red channel and AF signal intensity of the tumour was graded as hypo-, iso-, hyper-intense or mixed compared with the surrounding healthy tissue. The presence of subretinal fluid was noted as a haze reducing

Table 1. Tumour characteristics before and after radiotherapy.

	Pre-therapy	Post-therapy	p value
Presence of orange pigment	51%	46%	0.65
Presence of drusen	8%	10%	0.69
Presence of subretinal fluid			
Red channel	74%	62%	0.22
Pseudocolour	79%	74%	0.59
Autofluorescence	95%	92%	0.64
Intensity grade			
Red channel	Iso-intense 3% Hypo-intense 20% Mixed 77%	Iso-intense 3% Hypo-intense 15% Mixed 82%	0.83
Autofluorescence	Hypo-intense 3% Mixed 97%	Hypo-intense 5% Mixed 95%	0.55

detail recognition of the surrounding tissue around the tumour in the pseudo-colour and red channel mode, whereas it could be detected as an area of higher signal intensity in fundus autofluorescence (AF) (Figure 1). Subretinal fluid was always confirmed with spectral-domain optical coherence tomography (SD-OCT) to ensure accuracy. In pseudocolour, drusen and orange pigment on the tumour surface were documented as yellow and orange spots, respectively. The discrimination between bright-coloured drusen and other dark-coloured pigmentary changes showed no difficulty in pseudocolour. On the contrary, orange pigment (lipofuscin deposits) was difficult to detect in pseudo-colour images, thus we used AF, where it was intensely hyperautofluorescent. Tumour diameter was also evaluated in the pseudo-colour and red channel mode. Maximal initial diameter was chosen after measuring it in various axes, the maximal final diameter was measured in the same axis of the initial one. All mentioned parameters were graded by two observers independently (A.P. and G.B.). In case of disagreement, the patient would be excluded from the study. In addition, B-sonographic maximal mean tumour basal diameter and height before and after PBRT were documented.

Statistics and mathematical analyses

We performed all analyses using R version 3.4.2 (R core team, R foundation for statistical computing, Vienna, Austria; https://www.R-project.org; 2017) and MedCalc statistical software version 16.8.4 (MedCalc Software bvba, Ostend, Belgium; https://www.medcalc.org; 2016). Chi-square and Wilcoxon tests were performed to compare tumour characteristics before and after radiation. GraphPad Prism 7 (GraphPad Software Inc.2017, La Jolla, USA) was performed in paired analysis to compare maximal diameter in red channel mode and in pseudo-colour mode, as well as, to compare ultrasound basal diameter and ultrasound height before and after therapy. A 2-tailed p value of <0.05 was considered statistically significant for all tests.

Bland-Altman plot analysis was performed using MedCalc to compare the measurements of continuous variables between two methods.

Results

Our sample consisted of 23 men (61%) and 15 women (39%). Mean follow-up period was 24 months (standard deviation (SD): 12, range 6–48).

Median age was 60 years (range: 41–85). Almost 82% (31 of 38) of the patients had symptoms before seeking medical advice. The tumour was located post-equatorial in almost 90% and equatorial or pre-equatorial in 10% of the cases.

Median best-corrected visual acuity was initially 20/40 (range: 20/2000 to 20/20) compared with 20/63 (range: 20/2000 to 20/20) at the last follow-up examination after treatment. This difference was statistically significant (Wilcoxon signed-rank test, $p=0.001$). Radiation retinopathy, maculopathy and optic neuropathy were documented in 62%, 54% and 10% after therapy, respectively. Toxic tumour syndrome was documented in 10% of patients. All of them had subretinal fluid at presentation. Orange pigment was found in 51% ($n=20$) before and 46% ($n=18$) after PBRT; the difference was also not statistically significant (chi-square test, $p=0.651$). Drusen were found in 8% ($n=3$) and 10% ($n=4$) of cases pre- and post-therapy respectively (chi-square test, $p=0.692$).

Concerning the presence of subretinal fluid changes before PBRT it was noted in 79% of the pseudo-colour mode, in 74% of the red channel mode and in 95% of the AF mode. After therapy, the presence of subretinal fluid was noted in 74% of the pseudo-colour mode, in 62% of the red channel mode and in 92% of the AF mode. Neither in the pseudo-colour nor in the red channel or AF mode was the presence of subretinal fluid statistically significant before and after therapy (chi-square test: pseudo-colour $p=0.591$, red channel $p=0.225$, AF mode $p=0.644$).

Regarding the intensity grade in the red channel, 20% of the tumours were hypo-intense, 3% iso-intense and 77%

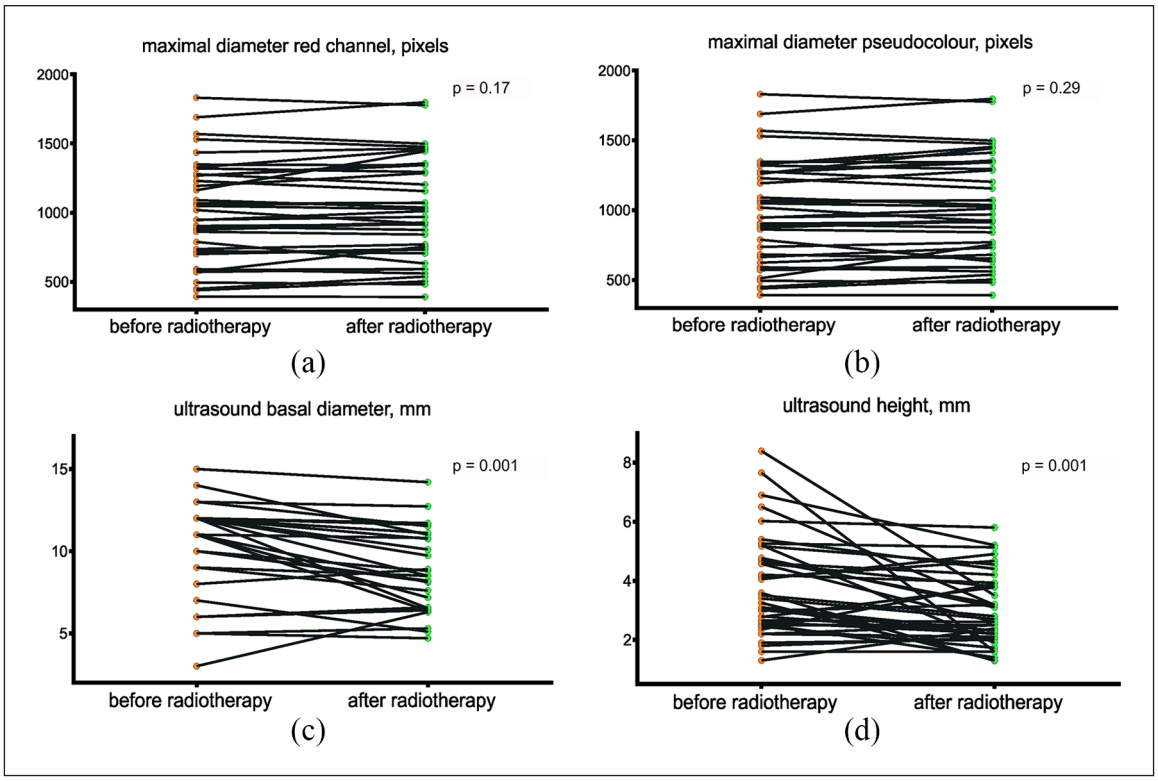

Figure 2. Paired analysis before and after radiotherapy for each patient: (a) maximal diameter in red channel mode (pixels), (b) maximal diameter in pseudo-colour mode (pixels), (c) ultrasound basal diameter (mm) and (d) ultrasound height (mm).

had mixed intensity at presentation. At the last follow-up visit, 15% were hypo-intense, 3% iso-intense and 82% had mixed intensity. In 95% of the cases the intensity grade remained unchanged before and after PBRT and the statistical difference pre- and post-therapy was not significant (chi-square test, $p=0.839$).

The AF intensity was in 3% hypo-intense and in 97% of the cases mixed before therapy, and in 5% hypo-intense and in 95% of the cases mixed after therapy. The intensity grade changed in only one patient; this difference was not statistically significant (chi-square test, $p=0.556$). The results are summarised in Table 1.

In the pseudo-colour mode, mean maximal tumour diameter was 989 (SD: 368) pixels before radiation and 994 (SD: 364) pixels at the last follow-up visit; this difference was not significant (Wilcoxon signed-rank test, $p=0.295$). In the red channel mode, mean maximal tumour diameter was 1008 (SD: 367) pixels at initial examination compared with 1012 (SD: 366) pixels after therapy, this was not statistically significant either (Wilcoxon signed-rank test, $p=0.174$) (Figure 2(a) and (b)).

In the ultrasound examination, the initial and the final mean tumour height were 3.88 mm (SD: 1.69) and 3.02 mm (SD: 1.19), respectively; this difference was statistically significant (Wilcoxon signed-rank test, $p=0.001$). The mean basal diameter was 9.7 mm (SD: 2.84) and 8.63 mm (SD: 2.59) at initial and last findings, respectively, which was statistically significant (Wilcoxon signed rank test, $p=0.001$) (Figure 2(c) and (d)).

The maximal diameter of the tumour in red channel mode was bigger than in the pseudo-colour mode before radiation in 13% of the cases (5 of 39). Because of the clinical importance of exactly defining tumour diameter and tumour borders before planning therapy, we further analysed this issue using the Bland-Altman plot (Figure 3). It was found that the diameter in the pseudo-colour channel mode was 0.9% smaller than in the red mode. Three outliers (8%) were outside the −1.96 SD and +1.96 SD range. The difference of measurements in these cases between pseudo-colour and red channel mode were +8%, –11% and –12%, respectively.

Discussion

The questions that this study is attempting to answer are on one hand, how the characteristics of uveal melanomas on Optos® are distributed before therapy and, on the other hand, how they change after therapy. There is no other study in the literature so far that compares the imaging characteristics using UWF-SLO before and after PBRT. This issue is crucial, because the clinician is confronted with the question if the therapy has been successful or not.

Despite its limitations compared with other fundus imaging systems,[15,17–21] such as pseudocolour instead of

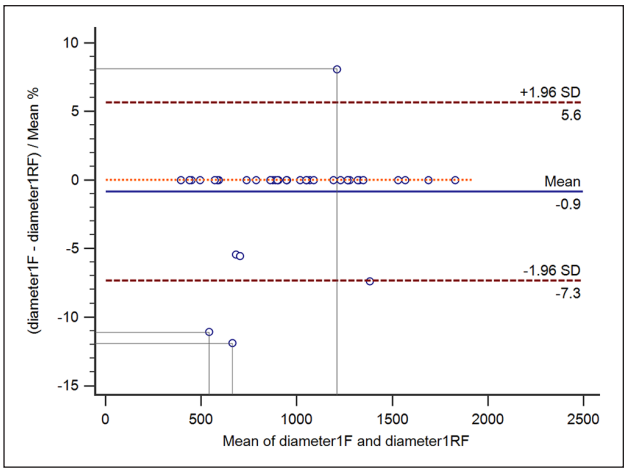

Figure 3. Bland-Altman plot of agreement between tumour maximum diameter in pseudocolour (1F) and in red channel (1RF) before treatment.

true colour imaging and the need for a dilated pupil to get good quality images of the fundus periphery, Optos has the advantage of ease of use and digital capturing, offering the opportunity to acquire within very short time ultra-wide-field fundus images collecting additional information depending on the wavelength used.

Apart from only one case of an iso-intense tumour in the red channel, in our results 100% and 97% of choroidal melanomas will be visible on the AF and the red channel, respectively, either as an area of mixed signal intensity or reduced intensity (Table 1). This makes the Optos also a valuable tool for screening purposes for choroidal melanocytic tumours. There was no significant change in the imaging pattern of most tumours in our study, such as from hypo-intense to mixed, for example. PBRT induces DNA damage to tumour cells and late apoptosis, in a pattern that is different than the radionecrosis induced by other radiation modalities. As a result, there are no significant retinal pigment epithelium (RPE) changes on or around the tumour seen after PBRT, in contrast to other radiation methods.[4] Clinicians should expect slight changes in the AF and red channel patterns during the follow-up period of uveal melanomas treated with PBRT, but the overall categorisation should remain the same. In a different scenario, suspicion for recurrence should be raised and the issue should be co-evaluated with other parameters, such as tumour growth.

Subretinal fluid in our study was confirmed with SD-OCT and equally often documented in the pseudo-colour and red channel mode. The easiest way to visualise it is nevertheless AF. One should keep in mind that the hypofluorescent changes seen in AF could either indicate subretinal fluid at the time point of the examination or diffuse damage of RPE after resorption of previously existing subretinal fluid.

It was found that cases with subretinal fluid accumulation initially had a higher probability of developing toxic tumour syndrome. This is in accordance with the observation that toxic tumour syndrome is expected in large tumours, which almost invariably present with an exudative retinal detachment of some extent.

In three cases (8%), we found substantial differences in the measurements between the pseudo-colour and red channel acquisitions. When performing treatment planning, this error can influence the size of designated target volume and thus treatment success. The red laser penetrates deeper into the retina and choroid. Consequently, in slightly pigmented or amelanotic choroidal lesions that are difficult to discern from the surrounding normal choroid, it delineates them with more precision without the negative green channel influence of the retinal surface. In two cases, the tumour diameter was measured 11% and 12% less in the pseudo-colour mode than in the red channel mode, respectively. With an average diameter of approximately 10 mm in our study population, 12% means a difference of over 1 mm. Taking into consideration that a safety margin of 2 mm is applied when radiating a tumour with protons, an underestimation of the tumour size via the pseudo-colour mode could lead to inadequate treatment and tumour recurrence. No patient had local tumour recurrence in our series. On the contrary, image sharpness can be slightly reduced in anterior parts of the lesion thus compromising the accuracy of the diameter measurements in the red channel mode. This can explain the discrepancy in the diameter measurements between the pseudo-colour and red channel mode in the single case where the tumour diameter in the former was larger than in the latter. Thus, it is advisable to use and compare both channels when determining tumour borders before therapy, in order to avoid mistakes.

Ultrasound examination is so far the ‘gold standard’ in following up uveal melanoma.[22,23] Although in our study, tumour diameter did not significantly change in Optos before and after therapy, it did so in the ultrasound examination. This initially paradoxical issue can be explained by the fact that Optos obtains an en-face image, whereas tumour diameter in the ultrasound is determined from the side, by putting the markers at the border of the elevation. As tumours shrink in height after PBRT, their sonographic diameter consequently decreases (like a melting iceberg with its diameter measured at sea level). The explanation for this is that tumour margins become thin enough not to show in ultrasound during tumour regression after PBRT, thus resulting in wrong sonographic diameter estimations.[24] Although ultrasound still remains the gold standard, new imaging technology is implemented in our everyday practice and knowledge gained can be intergraded in the follow-up protocols we have so far.

Limitations of the study

One of the drawbacks of this study is that it is retrospective and some of the characteristics that are being evaluated are qualitative. To overcome this issue, an agreement between

both observers in every characteristic was required for each case in order to be included in the study. Unfortunately, there is no qualified software at present that can objectively classify the tumours according to the qualitative characteristics that we evaluated. Should such a software protocol become available, this would greatly improve the objectivity of such measurements. Nevertheless, the main aim of the study was not to measure the absolute maximal diameter of the tumour, but to document the changes after PBRT. No significant changes were noted. A further possible weak point of this study is the great range in the follow-up period (6–48 months) as well as the fact that the post-treatment image was not taken at the same follow-up time point for all patients.

To conclude, Optos® wide-field imaging can be a substantial tool additionally to the gold standard techniques used so far, such as ultrasound, in the clinical evaluation of uveal melanomas before and after PBRT. Further studies are necessary to adequately evaluate the utility of this imaging option for intraocular malignancies.

Acknowledgements

The authors would like to thank Mr Peter Wolfgang and Dr Andre Viveiros for their assistance with statistical analysis in this study.

Declaration of conflicting interests

The author(s) declared no potential conflicts of interest with respect to the research, authorship and/or publication of this article.

Funding

The author(s) received no financial support for the research, authorship and/or publication of this article.

References

1. Kashyap S, Meel R, Singh L, et al. Uveal melanoma. *Semin Diagn Pathol* 2016; 33: 141–147.
2. Gragoudas ES, Goitein M, Verhey L, et al. Proton beam irradiation. An alternative to enucleation for intraocular melanomas. *Ophthalmology* 1980; 87(6): 571–581.
3. Egger E, Zografos L, Schalenbourg A, et al. Eye retention after proton beam radiotherapy for uveal melanoma. *Int J Radiat Oncol Biol Phys* 2003; 55(4): 867–880.
4. Groenewald C, Konstantinidis L and Damato B. Effects of radiotherapy on uveal melanomas and adjacent tissues. *Eye (Lond)* 2013; 27(2): 163–171.
5. Seidensticker F, Neubauer AS, Wasfy T, et al. Wide-field fundus autofluorescence corresponds to visual fields in chorioretinitis patients. *Clin Ophthalmol* 2011; 5: 1667–1671.
6. Schweitzer D, Schenke S, Hammer M, et al. Towards metabolic mapping of the human retina. *Microsc Res Tech* 2007; 70(5): 410–419.
7. Hammer M, Konigsdorffer E, Liebermann C, et al. Ocular fundus auto-fluorescence observations at different wavelengths in patients with age-related macular degeneration and diabetic retinopathy. *Graefes Arch Clin Exp Ophthalmol* 2008; 246(1): 105–114.
8. Croft DE, van Hemert J, Wykoff CC, et al. Precise montaging and metric quantification of retinal surface area from ultra-widefield fundus photography and fluorescein angiography. *Ophthalmic Surg Lasers Imaging Retina* 2014; 45(4): 312–317.
9. Oishi A, Hidaka J and Yoshimura N. Quantification of the image obtained with a wide-field scanning ophthalmoscope. *Invest Ophthalmol Vis Sci* 2014; 55(4): 2424–2431.
10. Kernt M, Schaller UC, Stumpf C, et al. Choroidal pigmented lesions imaged by ultra-wide-field scanning laser ophthalmoscopy with two laser wavelengths (Optomap). *Clin Ophthalmol* 2010; 4: 829–836.
11. Coffee RE, Jain A and McCannel TA. Ultra wide-field imaging of choroidal metastasis secondary to primary breast cancer. *Semin Ophthalmol* 2009; 24(1): 34–36.
12. Jain A, Shah SP, Tsui I, et al. The value of Optos Panoramic 200MA imaging for the monitoring of large suspicious choroidal lesions. *Semin Ophthalmol* 2009; 24(1): 43–44.
13. Heimann H, Jmor F and Damato B. Imaging of retinal and choroidal vascular tumours. *Eye (Lond)* 2013; 27(2): 208–216.
14. Zapata MA, Leila M, Teixidor T, et al. Comparative study between fundus autofluorescence and red reflectance imaging of choroidal nevi using ultra-wide-field scanning laser ophthalmoscopy. *Retina* 2015; 35(6): 1202–1210.
15. Nurnberg D, Seibel I, Riechardt AI, et al. Multimodale Bildgebung des Aderhautmelanoms mit seinen Differenzialdiagnosen, Therapie (Bestrahlungsplanung) und Verlaufskontrolle. *Klin Monbl Augenheilkd* 2018; 235: 1001–1012.
16. Oellers P, Lains I, Mach S, et al. Novel grid combined with peripheral distortion correction for ultra-widefield image grading of age-related macular degeneration. *Clin Ophthalmol* 2017; 11: 1967–1974.
17. Pomerantzeff O. Equator-plus camera. *Invest Ophthalmol* 1975; 14: 401–406.
18. Shields CL, Materin M and Shields JA. Panoramic imaging of the ocular fundus. *Arch Ophthalmol* 2003; 121(11): 1603–1607.
19. Pe'er J, Sancho C, Cantu J, et al. Measurement of choroidal melanoma basal diameter by wide-angle digital fundus camera: a comparison with ultrasound measurement. *Ophthalmologica* 2006; 220(3): 194–197.
20. Webb RH, Hughes GW and Delori FC. Confocal scanning laser ophthalmoscope. *Appl Opt* 1987; 26: 1492–1499.
21. Friberg TR, Pandya A and Eller AW. Non-mydriatic panoramic fundus imaging using a non-contact scanning laser-based system. *Ophthalmic Surg Lasers Imaging* 2003; 34(6): 488–497.
22. Ossoinig KC. Standardized echography: basic principles, clinical applications, and results. *Int Ophthalmol Clin* 1979; 19(4): 127–210.
23. Coleman DJ and Lizzi FL. Computerized ultrasonic tissue characterization of ocular tumors. *Am J Ophthalmol* 1983; 96(2): 165–175.
24. Rashid M, Heikkonen J and Kivela T. Tumor regression after brachytherapy for choroidal melanoma: reduction of thickness and cross-sectional area by shape and regression pattern. *Invest Ophthalmol Vis Sci* 2015; 56(4): 2612–2623.